

Photonic crystal light emitting diode based on Er and Si nanoclusters co-doped slot waveguide

R. Lo Savio,¹ M. Galli,¹ M. Liscidini,¹ L. C. Andreani,¹ G. Franzò,² F. Iacona,² M. Miritello,² A. Irrera,³ D. Sanfilippo,⁴ A. Piana,⁴ and F. Priolo^{2,5}

¹Dipartimento di Fisica, Università di Pavia, Via Bassi 6, 27100 Pavia, Italy

²MATIS-IMM CNR and Dipartimento di Fisica e Astronomia, Università di Catania, via S. Sofia 64, 95123 Catania, Italy

³CNR-IPCF, Viale Ferdinando Stagno d'Alcontres 37, 98158 Messina, Italy

⁴ST Microelectronics, Stradale Primosole 50, 95121 Catania, Italy

⁵Scuola Superiore di Catania, Università di Catania, Via Valdisavoia 9, 95123 Catania, Italy

(Received 22 October 2013; accepted 16 March 2014; published online 25 March 2014)

We report on the design, fabrication, and electro-optical characterization of a light emitting device operating at 1.54 μm , whose active layer consists of silicon oxide containing Er-doped Si nanoclusters. A photonic crystal (PhC) is fabricated on the top-electrode to enhance the light extraction in the vertical direction, and thus the external efficiency of the device. This occurs if a photonic mode of the PhC slab is resonant with the Er emission energy, as confirmed by theoretical calculations and experimental analyses. We measure an increase of the extraction efficiency by a factor of 3 with a high directionality of light emission in a narrow vertical cone. External quantum efficiency and power efficiency are among the highest reported for this kind of material. These results are important for the realization of CMOS-compatible efficient light emitters at telecom wavelengths.

© 2014 AIP Publishing LLC. [<http://dx.doi.org/10.1063/1.4869751>]

Er-doped Si nanoclusters embedded in a SiO_2 matrix is a widely studied material for the development of light emitting devices operating at room temperature at 1.54 μm , which represents a strategic wavelength for applications in Si-photonics and optoelectronics, and more generally for telecommunications.¹ In this material, Si nanoclusters (Si-nc) can be excited by an external source (for example a visible photon or an electron), and then can transfer the absorbed energy to the surrounding Er ions.^{2–4} Once excited, the Er ions may radiatively decay emitting photons at 1.54 μm , generated by the transition between the first excited $^4I_{13/2}$ level and the ground state $^4I_{15/2}$ of the rare-earth. The sensitization effect of Si-nc is highly efficient, allowing to increase the excitation cross section of Er in SiO_2 from 10^{-21} cm^2 up to 10^{-16} cm^2 when Si-nc are present.^{5,6} Moreover, Si nanoclusters can be also electrically excited, thus allowing the fabrication of electroluminescent devices working at room temperature.^{7–9} In 2010, Jambois and co-workers demonstrated a Er:Si-nc: SiO_2 device in which 20% of total Er atoms in the active material was excited; in spite of the very high excited Er fraction, close to the inversion population threshold, the reported external quantum efficiency (EQE) and power efficiency (PE) were 0.4% and 0.01%, respectively.¹⁰ Moreover, a recent report on electrically driven Er-doped slot waveguides, having Er ions and Si nanoclusters in the active region, reports a power efficiency even lower ($10^{-4}\%$) due to the propagation losses.¹¹ As a consequence of intrinsically low power efficiency as well as unfavourable emission pattern, such devices cannot be still proposed for practical applications.

A major drawback in semiconductor-based Light Emitting Devices (LED) is that most of the light generated by the active material is trapped inside the device by total internal reflection; therefore, one possible way to increase the efficiency is to enhance the fraction of light escaping the

device in the vertical direction. This can be achieved, for example, through the fabrication of a planar 2D photonic crystal, as first proposed in Ref. 12, and recently reviewed in Ref. 13. The simultaneous enhancement of Er photoluminescence and the redistribution of emitted light in the vertical direction were demonstrated in horizontal PhC slot waveguides containing an active Er:Si-nc layer.¹⁴ The same approach was also exploited to demonstrate the enhancement of electroluminescence emission in the 700–1100 nm range in a device containing only Si-nc (without Er atoms) as emitting material.¹⁵ Furthermore, the slot geometry used gives a double advantage of enhancing the electromagnetic field in the active material,¹⁶ and yielding a very convenient configuration for electrical pumping.

In this letter, we demonstrate an Er:Si-nc co-doped LED with a slot waveguide structure that operates at 1.54 μm and at room temperature with a proper PhC designed and patterned on the top electrode. Thanks to the photonic structure the Er emission in the vertical direction, and then the external efficiency of the LED, is 3-fold increased due to a contemporary increase of the extraction efficiency in air (η_{extr}) and an angular redistribution of the emitted light towards a narrow cone in the vertical direction.

The fabrication of the device starts with the deposition by low pressure chemical vapour deposition (LPCVD) of a 110 nm thick polycrystalline Si film on top of a 1.9 μm thick SiO_2 layer, thermally grown on a 6 in. Si wafer. This Si layer, after being doped with boron by ion implantation, acts as the lower electrode of the device. The Er-doped SiO_x active layer (50 nm thick) is then deposited by reactive co-sputtering of Si and Er_2O_3 targets, in a reactive atmosphere consisting of a mixture of Ar and O_2 gases (more details can be found in Ref. 17). The total Si concentration in the film was 37 at. %, corresponding to an excess of about 6

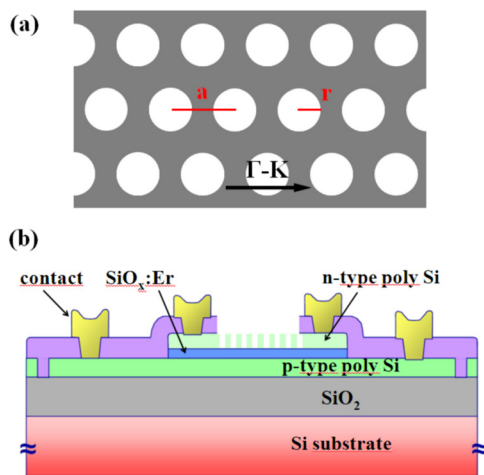


FIG. 1. (a) Top and (b) side schematic view of the PhC slot waveguide.

at. %, and the Er concentration was 2×10^{20} at./cm³, as verified by Rutherford backscattering spectrometry. After the deposition, the films were annealed at 900 °C for 1 h in N₂ atmosphere to optically activate Er and to induce the phase separation between Si and SiO₂ with the formation of Er-doped amorphous Si nanoclusters.¹⁸ At the same time, the thermal process enables the diffusion and the electrical activation of B inside the polycrystalline Si layer. Previous results demonstrated that reactive co-sputtering technique allows the formation of an almost stoichiometric high quality SiO₂ layer, embedding both Er and Si-nc, leading to efficient and stable LEDs.¹⁷ The upper electrode is then formed through the deposition of a 115 nm thick Si layer by LPCVD followed by As implantation, and a thermal treatment at 1000 °C for 30 s to electrically activate the n-dopant. Thickness and refractive index of the three layers were evaluated by spectroscopic ellipsometry; the thickness variation of the three deposited layers all over the 6 in. wafer surface is below 5%, and the refractive index of the active layer (Er:Si-nc:SiO₂) is 1.49 ± 0.01 .

The active area of the device ($100 \times 100 \mu\text{m}^2$) was defined by photolithography, and then metal Al/Cu/Si rings were deposited to form the electrical contacts. Finally, a PhC is locally patterned on the active area of the devices by means of electron beam lithography and reactive ion etching processes. The PhC consists of a triangular lattice of air holes, as schematically sketched in Fig. 1(a). The lattice constant a and the normalized hole radius (r/a) are 750 nm and 0.33, respectively, as determined on the basis of the theoretical calculations reported in the following. The depth of the holes is 110 nm, corresponding to the thickness of the top Si layer. Reference devices were also fabricated without patterning the top Si electrode. The vertical structure of the device is schematically shown in Fig. 1(b).

The PhC patterned on the top electrode has been carefully designed in order to maximize the extraction of the light emitted by Er atoms in the vertical direction. We calculated the photonic band structure for PhC slabs for different lattice constants using the method of expansion on the guided modes of an effective waveguide.¹⁹ Figs. 2(a)–2(d) report the photonic modes of four PhC slot waveguides with $r/a=0.33$ and lattice constant a varying between 740 and 800 nm along the Γ -K direction. An optically active photonic

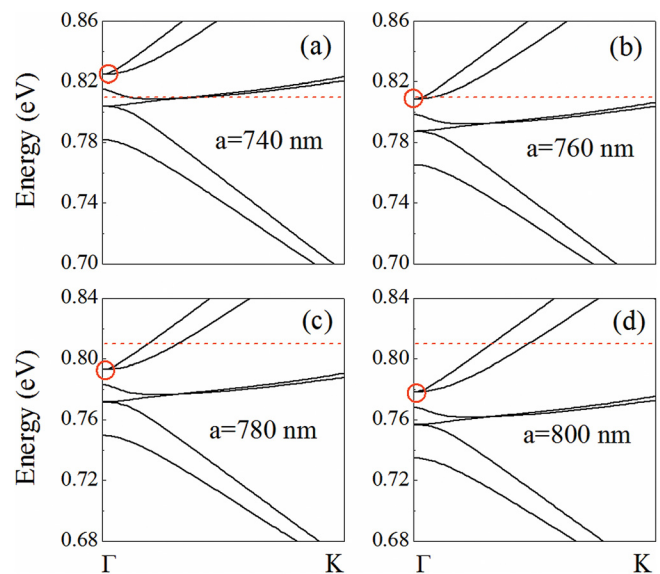


FIG. 2. (a)–(d) Photonic band dispersions calculated for PhC having different parameters. The red circle highlights the photonic mode closest to Er energy emission, indicated by a red dashed line.

mode, highlighted by a red circle in the figure, close to the emission energy of Er, peaked at 0.81 eV, is clearly visible; it is degenerate at Γ and splits into two modes of opposite parities along the Γ -K direction. Maximum light emission in the vertical direction occurs when the photonic mode is resonant with Er emission energy at Γ point; this condition is achieved when a is between 740 and 760 nm.

Photoluminescence (PL) analyses were performed to measure the Er emission under optical pumping in devices with different PhCs; a 640 nm laser was used as excitation source. Since the optical pump energy is well above the photonic band gap of the PhCs, we are confident that the excitation efficiency is not influenced by the photonic structures. Maximum PL intensity was observed for lattice constant of 750 nm (data not shown), confirming the calculations. Therefore, in the following we will focus our attention only on this device. Finally, we also calculated η_{extr} in this structure, concluding that 26% of light generated inside the device is emitted in air.²⁰ This is close to the value (20%) estimated from the theory of Ref. 21, which can be applied by treating the patterned Si layer in the effective-index approximation.

Figure 3(a) shows a top view image of the patterned device obtained by scanning electron microscopy (SEM) with a

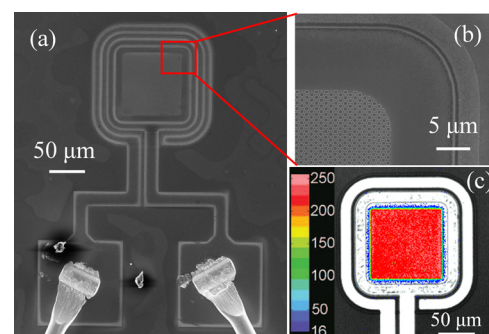


FIG. 3. (a) Top-view SEM image of one device. (b) Detailed SEM image of the top-right part of the device, highlighting the patterned PhC. (c) EmMi image of one device under forward polarization; the image is in false colors, red corresponding to more intense EL signal.

field emission Zeiss Supra 25 microscope; the two metal rings acting as electrical contacts to the top n-type Si and to the bottom p-type Si are clearly visible. The wide central area of the device is free of any metallization to allow the exit of the light and preserve the properties of the photonic structure. A more detailed image of the PhC patterned on the top electrode is shown in Fig. 3(b), where good uniformity of the hole shape, size, and spacing are evident. When the device is biased with an external direct voltage source, a current flow is established between the two electrodes; carriers flowing through the thin active layer by tunnelling excite the Si-nc that then transfers the energy to surrounding Er atoms that finally emit photons at $1.54 \mu\text{m}$.⁹

Electroluminescence (EL) of the devices was first investigated by emission microscopy (EmMi), using an optical microscope coupled to an InGaAs charged coupled device camera that allows the detection of infrared light emitted under the application of an external voltage. Fig. 3(c) shows an EmMi image taken at room temperature, by biasing the device with a 39 V voltage source, causing a current flow of 100 nA passing through the structure. Bright and uniform EL originates from the whole active area, indicating that Er ions are excited under polarization. Moreover, it is worth noticing the absence of hot spots and/or depolarized regions, confirming the effectiveness of the top electrode design. An interesting feature can be noticed by observing one of the four corners of the device, both by SEM and by EmMi images. In fact, in Fig. 3(c) the presence of a small blue coloured edge region is evident, where the EL intensity is lower as compared to the central region of the device. The correlation between the step-like variation of the EL intensity and the end of the PhC pattern, as identified in the SEM image of the same corner, is impressive. This is a clear evidence of the effectiveness of the PhC in enhancing light extraction from this device.

Angle-resolved EL measurements were carried on by biasing the devices through a variable voltage generator. The light emitted by the device was collected by means of a microscope objective (NA = 0.4, working distance 15 mm) focused on the device; an iris was placed in front of the objective to reduce the collection angle. The angle resolution of the optical setup is about 2° . The angle between the collection path and the sample was varied between 0° and 80° . Finally, collected light was sent to a grating spectrometer coupled to a liquid-nitrogen cooled InGaAs array detector. In Fig. 4, we report the EL spectrum of the patterned LED taken in the vertical direction (assumed as 0°) under a current of 50 nA, as compared to the EL spectrum of the unpatterned device under the same flowing current. Both spectra show the typical Er emission lineshape, and in both cases no signal was detected in other spectral regions, confirming that the spatial correlation between EL enhancement and presence of PhC observed by EmMi (Fig. 3(c)) is entirely due to the Er emission enhancement. A 3-fold enhancement of EL integrated over the Er lineshape is observed in the PhC device. The enhancement is weakly wavelength-dependent, being almost constant (included between 3 and 3.5) in the narrow spectral region where the Er emission is more intense.²⁰

Fig. 4(b) shows the polar distribution of the integrated EL signal obtained for different emission angles in un-patterned

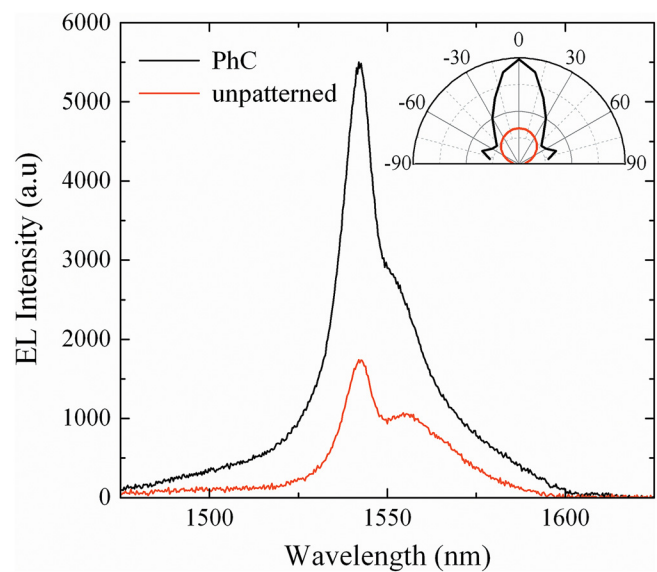


FIG. 4. EL spectra collected at vertical direction of the PhC-patterned device and an un-patterned one under the same flowing current of 50 nA. Polar distribution of the integrated Er emission for the same devices is shown in the inset.

and patterned devices. As expected, the former exhibits a cosine-like distribution characteristic of emission in random directions; on the other side the emission pattern from the PhC device is directional, showing a pronounced emission peak in the vertical direction, and a secondary peak for emission angles around 70° . The main peak is attributed to the dipole-allowed photonic mode at the Γ point, as shown in Fig. 2, while the secondary peaks are due to higher-order photonic modes at large wavevectors (outside the range of Fig. 2). The results reported here show the double beneficial effect of PhC, increasing the fraction of light emitted in the air cladding, and spatially redistributing the light emitted with a stronger enhancement in the vertical direction.

Starting from EL measurements we estimated also the optical power. In Fig. 5, we report the EL spectra obtained for different currents passing through the device, by collecting the Er emission with a high NA microscope objective (NA = 0.8), and focusing it to the entrance slit of a grating spectrometer equipped with an InGaAs array detector. In order to convert the EL intensity, given by the number of

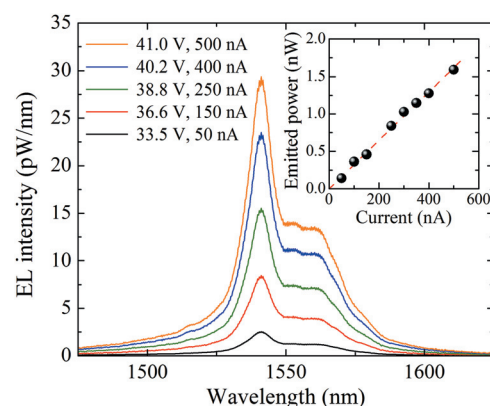


FIG. 5. EL spectra of the device observed for different currents; the spectral power density is extracted starting from the raw values of the emitted power. Trend of corrected emitted power is reported in the inset; dashed red line is a guide to the eye.

counts in the InGaAs detector, into a value of real emitted power, we recorded also the power emitted for each input current by focusing the light onto a high-sensitivity InGaAs power meter. The maximum measured power was 0.88 nW, under a bias voltage of 41 V and a flowing current of 500 nA. This high voltage value is typical of Er:Si-nc LEDs, due to tunnelling of electrons through the insulating barrier in order to excite Si nanoclusters, and comparable with values reported in literature.^{7–11,17} Starting from the emitted power values, we can convert the EL intensity into a spectral power density, as shown in the vertical axis of Figure 5.

The raw measured value must be corrected taking into account the collection efficiency and the losses of the optical system that collects the light. The former can be estimated considering that only the photons emitted at angles lower than $\sin^{-1}(NA/n) = \sin^{-1}(0.8) = 53^\circ$ are collected by the objective; from angle-resolved EL data shown in Fig. 4(b), we can estimate that 85% of light is collected. It is remarkable to underline again that almost all the emitted light can be experimentally collected by using a high-NA objective. This is a definite advantage of using a PhC to improve directionality of light emission. The absorption losses due to the setup were estimated through a direct measurement of the transmission coefficient of a 1540 nm laser, yielding 65%. Therefore, a correction factor $(0.85 \times 0.65)^{-1}$ must be applied to the raw data. The corrected power as a function of I is shown in the inset of Fig. 5, exhibiting a linear trend; the maximum power emitted is 1.6 nW, under a bias voltage of 41 V and a flowing current of 500 nA. Starting from these numbers, we can estimate the efficiency of the device. The EQE, defined as the ratio between the number of emitted photons and the number of injected carriers, is 0.4%, while the PE, defined as the ratio between the optical emitted power and the electrical input power is 0.01%. These values are at the highest levels reported in the literature for Er-doped Si-based devices.

Further improvements could be achieved by extracting the light emitted downward, corresponding to the 74% of the overall light generated inside the device, by means of a suitable dielectric back-reflector. This solution could be very advantageous in the device structure proposed here since the back-reflected light would be efficiently extracted in the vertical direction by the PhC. In this way, the device efficiency could be increased by a factor of 4. Therefore, engineering this kind of LED through the use of a slot waveguide geometry and the fabrication of photonic structures to enhance the light extraction is a valuable strategy towards possible applications.

In conclusion, we have demonstrated a slot waveguide LED operating at 1.54 μm , whose active layer is formed by a SiO₂ film co-doped with Er and Si nanoclusters, showing an enhancement of the extraction efficiency in air and a spatial redistribution of light emitted through the patterning of a

PhC on the top-electrode. A 3-fold increase of EL emission and a strong narrowing of the emission cone are experimentally observed. Finally, external efficiency was estimated, yielding 0.4% and 0.01% for EQE and PE, respectively. This approach is very promising for Er:Si-nc based LED emitting at telecom wavelengths, with margins of improvements which could make it suitable for applications.

The authors are grateful to C. Creatore and M. Belotti for participating in the early stages of this work and for helpful discussions. This work has been performed within the framework of the FAR Project ‘‘Silicon Laser’’ (Grant No. 851/DSPAR/2003) funded by MIUR.

- ¹F. Priolo, T. Gregorkiewicz, M. Galli, and T. F. Krauss, *Nat. Nanotechnol.* **9**, 19 (2014).
- ²A. J. Kenyon, P. F. Trwoga, M. Federighi, and C. W. Pitt, *J. Phys.: Condens. Matter* **6**, L319 (1994).
- ³M. Fujii, M. Yoshida, Y. Kanzawa, S. Hayashi, and K. Yamamoto, *Appl. Phys. Lett.* **71**, 1198 (1997).
- ⁴G. Franzò, V. Vinciguerra, and F. Priolo, *Appl. Phys. A* **69**, 3 (1999).
- ⁵F. Priolo, G. Franzò, D. Pacifici, V. Vinciguerra, F. Iacona, and A. Irrera, *J. Appl. Phys.* **89**, 264 (2001).
- ⁶A. J. Kenyon, C. E. Chryssou, C. W. Pitt, T. Shimizu-Iwayama, D. E. Hole, N. Sharma, and C. J. Humphreys, *J. Appl. Phys.* **91**, 367 (2002).
- ⁷F. Iacona, D. Pacifici, A. Irrera, M. Miritello, G. Franzò, F. Priolo, D. Sanfilippo, G. Di Stefano, and P. G. Fallica, *Appl. Phys. Lett.* **81**, 3242 (2002).
- ⁸A. Nazarov, J. M. Sun, W. Skorupa, R. A. Yankov, I. N. Osiyuk, I. P. Tjagulskii, V. S. Lysenko, and T. Gebel, *Appl. Phys. Lett.* **86**, 151914 (2005).
- ⁹F. Iacona, A. Irrera, G. Franzò, D. Pacifici, I. Crupi, M. Miritello, C. D. Presti, and F. Priolo, *IEEE J. Sel. Top. Quantum Electron.* **12**, 1596 (2006).
- ¹⁰O. Jambou, F. Gourbilleau, A. J. Kenyon, J. Montserrat, R. Rizk, and B. Garrido, *Opt. Express* **18**, 2230 (2010).
- ¹¹A. Tengattini, D. Gandolfi, N. Prtljaga, A. Anopchenko, J. M. Ramirez, F. F. Lupi, Y. Berencén, D. Navarro_Urrios, P. Rivallin, K. Surana, B. Garrido, J.-M. Fedeli, and L. Pavesi, *J. Lightwave Technol.* **31**, 391 (2013).
- ¹²S. Fan, P. R. Villeneuve, J. D. Joannopoulos, and E. F. Schubert, *Phys. Rev. Lett.* **78**, 3294 (1997).
- ¹³A. David, H. Benisty, and C. Weisbuch, *Rep. Prog. Phys.* **75**, 126501 (2012).
- ¹⁴M. Galli, A. Politi, M. Belotti, D. Gerace, M. Liscidini, M. Patrini, L. C. Andreani, M. Miritello, A. Irrera, F. Priolo, and Y. Chen, *Appl. Phys. Lett.* **88**, 251114 (2006).
- ¹⁵C. D. Presti, A. Irrera, G. Franzò, I. Crupi, F. Priolo, F. Iacona, G. Di Stefano, A. Piana, D. Sanfilippo, and P. G. Fallica, *Appl. Phys. Lett.* **88**, 033501 (2006).
- ¹⁶M. Galli, D. Gerace, A. Politi, M. Liscidini, M. Patrini, L. C. Andreani, A. Canino, M. Miritello, R. Lo Savio, A. Irrera, and F. Priolo, *Appl. Phys. Lett.* **89**, 241114 (2006).
- ¹⁷A. Irrera, F. Iacona, G. Franzò, M. Miritello, R. Lo Savio, M. E. Castagna, S. Coffa, and F. Priolo, *J. Appl. Phys.* **107**, 054302 (2010).
- ¹⁸G. Franzò, S. Boninelli, D. Pacifici, F. Priolo, F. Iacona, and C. Bongiorno, *Appl. Phys. Lett.* **82**, 3871 (2003).
- ¹⁹L. C. Andreani and D. Gerace, *Phys. Rev. B* **73**, 235114 (2006).
- ²⁰See supplementary material at <http://dx.doi.org/10.1063/1.4869751> for details about calculations of the extraction efficiency and about the dependence of EL enhancement for different wavelengths.
- ²¹C. Creatore and L. C. Andreani, *Phys. Rev. A* **78**, 063825 (2008).